Phys Chem Minerals
DOI 10.1007/s00269-015-0794-1

ORIGINAL PAPER

Equation of state of synthetic qandilite Mg_2TiO_4 at ambient temperature

Mingda Lv[1,2] · Xi Liu[1,2] · Sean R. Shieh[3] · Tianqi Xie[3] · Fei Wang[1,2] · Clemens Prescher[4] · Vitali B. Prakapenka[4]

Received: 22 September 2015 / Accepted: 17 December 2015

Abstract Using a diamond-anvil cell and synchrotron X-ray diffraction, the compressional behavior of a synthetic qandilite $Mg_{2.00(1)}Ti_{1.00(1)}O_4$ has been investigated up to about 14.9 GPa at 300 K. The pressure–volume data fitted to the third-order Birch–Murnaghan equation of state yield an isothermal bulk modulus (K_{T0}) of 175(5) GPa, with its first derivative K'_{T0} attaining 3.5(7). If K'_{T0} is fixed as 4, the K_{T0} value is 172(1) GPa. This value is substantially larger than the value of the adiabatic bulk modulus (K_{S0}) previously determined by an ultrasonic pulse echo method (152(7) GPa; Liebermann et al. in Geophys J Int 50:553–586, 1977), but in general agreement with the K_{T0} empirically estimated on the basis of crystal chemical systematics (169 GPa; Hazen and Yang in Am Miner 84:1956–1960, 1999). Compared to the K_{T0} values of the ulvöspinel (Fe_2TiO_4; ~148(4) GPa with $K'_{T0} = 4$) and the ringwoodite solid solutions along the Mg_2SiO_4–Fe_2SiO_4 join, our finding suggests that the substitution of Mg^{2+} for Fe^{2+} on the T sites of the 4–2 spinels can have more significant effect on the K_{T0} than that on the M sites.

✉ Xi Liu
xi.liu@pku.edu.cn

[1] Key Laboratory of Orogenic Belts and Crustal Evolution, MOE, Peking University, Beijing 100871, People's Republic of China

[2] School of Earth and Space Sciences, Peking University, Beijing 100871, People's Republic of China

[3] Department of Earth Sciences, University of Western Ontario, London, ON N6A 5B7, Canada

[4] Center for Advanced Radiation Sources, University of Chicago, Chicago, IL 60439, USA

Keywords Compressibility · Diamond-anvil cell · Synchrotron X-ray diffraction · Qandilite

Introduction

Qandilite (ideally Mg_2TiO_4), a very rare 4–2 spinel, was first discovered from the periclase-forsterite marble wall rock of a shallow-seated alkaline-ultramafic intrusion in the Kangerdlugssuaq region of East Greenland (Gittins et al. 1982). It was later found in and named after the Qandil Group of metamorphic rocks (forsterite-rich Cretaceous calcareous sediments in contact with a kaersutite-rich banded diorite) at Dupezeh Mountain, Qala-Dizeh region, Iraq (Al-Hermezi 1985). Its field occurrences are seemingly restricted to some high-temperature magnesian skarns such as the contact zone of the Kondyor alkaline-ultramafic massif in Russia (Oktyabrsky et al. 1992), the metamorphosed siliceous dolomite xenoliths in a granite from the Ballachulish igneous complex, Scotland (Ferry 1996), and the forsterite-spinel-calcite skarn ejecta from Mt. Vesuvius, Italy (Pascal et al. 2011). As an end member of the ulvöspinel (Fe_2TiO_4)-qandilite series, which in turn belongs to the Fe_2TiO_4–Mg_2TiO_4–$FeFe_2O_4$–$MgFe_2O_4$ spinel quadrilateral, qandilite may be an important petrogenetic indicator of temperature and pressure for some geological processes (Ferry 1996). Therefore, many experimental studies have been conducted to investigate its physical and chemical properties (e.g., Wechsler and Navrotsky 1984; O'Neill et al. 2003; O'Neill and Scott 2005; Harrison et al. 2013; Bosi et al. 2014).

The crystal structure of qandilite has been studied by powder neutron diffraction, powder X-ray diffraction, and single-crystal X-ray diffraction (Wechsler and Von Dreele 1989; Millard et al. 1995; Sawada 1996). It is

Published online: 08 January 2016

an inverse spinel structure with the structural formula as $^{T}(Mg^{2+})^{M}(Mg^{2+}Ti^{4+})O_4$ (T, tetrahedral sites; M, octahedral sites), meaning Mg on both the T sites and M sites, and Ti on the M sites only. Redistribution of the Mg and Ti cations between the T and M sites only commences at around 1173 K, and its extent is very limited, so that qandilite can be approximated as an inverse 4–2 spinel (O'Neill et al. 2003; Palin et al. 2008; Harrison et al. 2013). The thermal expansivity of qandilite has been determined in O'Neill et al. (2003), and the free energy of formation has been measured in O'Neill and Scott (2005). The adiabatic bulk modulus (K_{S0}) of qandilite was constrained as 152(7) GPa by some ultrasonic velocity data up to 0.75 GPa (Liebermann et al. 1977), which was unfortunately too different to an empirical estimate of the isothermal bulk modulus (K_{T0} = 169 GPa; Hazen and Yang 1999). According to Liu et al. (2015), the difference between the K_{S0} and K_{T0} of any 4–2 spinel should be in the range of ~4 GPa [$(K_{S0}-K_{T0}) = \alpha\gamma TK_{T0}$, where α is the volumetric thermal expansion coefficient and γ is the Grüneisen parameter].

In this study, we have investigated the equation of state (EoS) of a synthetic qandilite at ambient temperature by using a diamond-anvil cell, coupled with synchrotron X-ray radiation.

Experimental method

The chemicals used to prepare the synthetic qandilite were MgO (99.99 %, Alfa Aesar) and TiO_2 (99.9 %, Alfa Aesar). These chemicals were firstly dried at 1373 K for 24 h to remove moisture absorbed from air, secondly weighed in an appropriate proportion corresponding to the chemical formula Mg_2TiO_4, then ground and homogenized manually in an agate mortar under acetone, and finally pressed into a pellet. This pellet was placed in a platinum crucible and sintered with a high-temperature furnace in open air. The sample was heated at 1673 K for 52 h and slowly cooled to room temperature at the rate of −5 K/min. One part of the pellet was crushed into fine powder for later X-ray diffraction experiments both at ambient pressure and at high pressure, and another part of the pellet was mounted in epoxy and polished using a series of diamond pastes. We characterized this material by using optical microscope, scanning electron microscope (SEM; FEI Quanta 650 FEG), EMPA (JEOL JXA-8100), and powder X-ray diffraction (XRD; X'Pert Pro MPD system; Hu et al. 2011) at ambient *P–T* conditions.

In situ high-pressure synchrotron X-ray diffraction experiments using a symmetrical diamond-anvil cell were performed at the beamline 13-ID-D of the GSECARS, Advanced Photon Source (APS), Argonne National Laboratory. The experimental techniques were similar to those used in our previous studies (Liu et al. 2009, 2011; Chang et al. 2013). Briefly, the powder sample was loaded into a rhenium gasket with a hole of 100 μm in diameter. Neon was used as the pressure-transmitting medium to minimize the deviatoric stress inside the sample chamber (Klotz et al. 2009). A ruby sphere was used as the pressure marker, and the ruby fluorescence method was used to determine the pressure (Mao et al. 1978). The incident synchrotron radiation beam was monochromatized to a wavelength of 0.3344 Å, and its beam size was collimated to ~3 × 4 μm^2. Each X-ray diffraction image was collected for about 30–120 s using an online CCD detector, and subsequently, the two-dimensional image was integrated to derive the one-dimensional X-ray diffraction pattern by using the Dioptas program (Prescher and Prakapenka 2015). The sample-to-detector distance (196.1654 mm) and the orientation of the detector were calibrated by using LaB_6. The XRD data were processed by using the PeakFit V4.12 software (SPSS Inc). The unit-cell parameters of the qandilite at different pressures were obtained by using the UnitCell program (Holland and Redfern 1997).

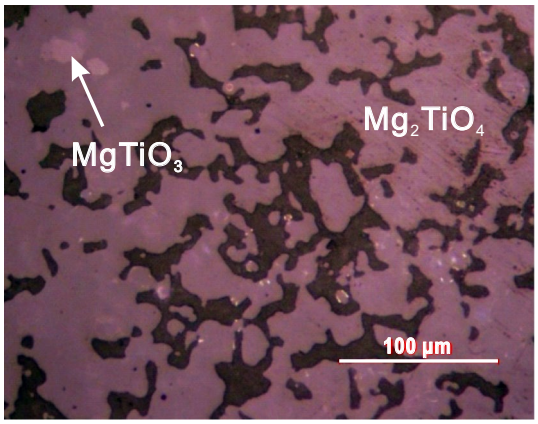

Fig. 1 Typical optical microscopic photograph of synthetic qandilite, coexisting with a small amount of geikielite. Irregular dark material is epoxy

Results and discussion

Our electron backscatter images and optical microscopic photographs (Fig. 1) show that the synthetic product mainly consists of two crystalline phases, with grain sizes ranging from 40 to 50 μm. The EMPA data suggest a chemical formula of $Mg_{2.00(1)}Ti_{1.00(1)}O_4$ (10 analyses) for the major phase and a chemical formula of $Mg_{1.00(2)}Ti_{1.00(1)}O_3$ (10 analyses) for the minor phase (<~5 %), which match the composition of qandilite and geikielite, respectively. The X-ray data at room *P–T* condition indicate that the major phase has the structure of qandilite whereas the

minor phase attains the structure of geikielite. According to O'Neill et al. (2003), qandilite is an ordered inverse 4–2 spinel and has very limited cation redistribution at high temperatures: At 1673 K (exactly the synthesizing temperature of our sample), only ~4 % Ti is present on the tetrahedral sites. We ignore any potential effect of this amount of cation disordering on our experimental result.

According to Akimoto and Syono (1967), Mg_2TiO_4 qandilite is presumably not a thermodynamically stable phase at high pressures and room temperature and should break down to MgO (periclase) + $MgTiO_3$ (geikielite). Our high-*P* experiments were conducted up to ~14.9 GPa at room temperature and did not show any sign of decomposition of the Mg_2TiO_4 qandilite, which was a typical kinetic issue. In total, we collected 17 X-ray diffraction patterns. Typical X-ray diffraction patterns are shown in Fig. 2. As pressure increased, all the peaks shifted continuously toward higher 2θ angles, but the overall X-ray diffraction pattern did not change. No apparent peak-broadening, no peak-splitting, and no new peaks were observed in our experiments.

The powder X-ray diffraction pattern at ambient pressure gives out the unit-cell parameters of the synthetic qandilite as $a_0 = 8.446(2)$ Å and $V_0 = 602.58(49)$ Å^3, in good agreement with the most recent observations ($a_0 = 8.44183(3)$ Å, Millard et al. 1995; $a_0 = 8.4443(4)$ Å and $V_0 = 602.13(8)$ Å^3, Sawada 1996; $a_0 = 8.4419(2)$ Å, O'Neill et al. 2003). Slight differences in chemical compositions or crystal structures (such as disordering magnitude) caused by different synthesizing conditions like varying temperatures and employment of a flux or not or in the setups of the X-ray diffraction experiments (Fleet et al. 2010) are presumably the sources for the extremely small fluctuations of the unit-cell parameters at ambient *P*–*T* condition.

The effect of pressure on the unit-cell volume of the qandilite is summarized in Table 1 and graphically shown in Fig. 3. A small nonlinear dependence on pressure over the investigated pressure range has been observed for the unit-cell volume.

In order to determine the isothermal bulk modulus of the qandilite, the *P*–*V* data have been fitted to the third-order Birch–Murnaghan equation of state (Birch 1947) by a least-squares method:

$$P = \left(\frac{3}{2}\right) K_{T0} \left[\left(\frac{V_0}{V}\right)^{\frac{7}{3}} - \left(\frac{V_0}{V}\right)^{\frac{5}{3}}\right] \times \left\{1 + \frac{3}{4}\left(K'_{T0} - 4\right)\left[\left(\frac{V_0}{V}\right)^{\frac{2}{3}} - 1\right]\right\},$$

where P is the pressure, K_{T0} the isothermal bulk modulus, K'_{T0} the first pressure derivative of K_{T0}, V_0 the volume at zero pressure, and V the volume at high pressure. The obtained parameters are $K_{T0} = 175(5)$ GPa, $K'_{T0} = 3.5(7)$, and $V_0 = 603.10(25)$ Å^3. When K'_{T0} fixed as 4, we have obtained $K_{T0} = 172(1)$ GPa and $V_0 = 603.21(18)$ Å^3 (second-order Birch–Murnaghan equation of state then).

The quality of the derived Birch–Murnaghan equation of state for qandilite can be evaluated by using a linear fitting

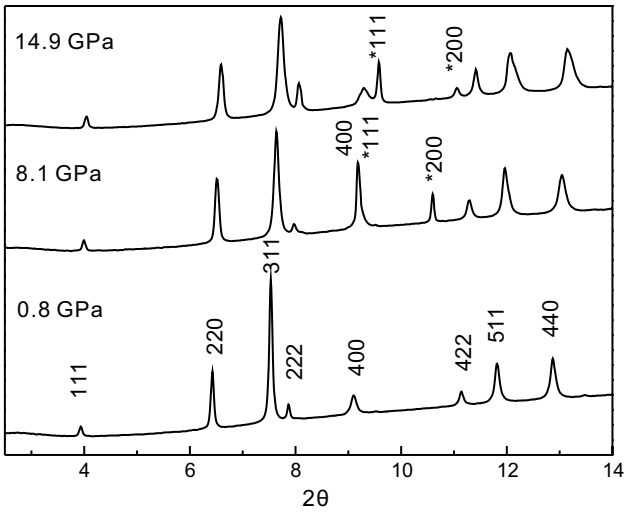

Fig. 2 Examples of X-ray diffraction patterns of qandilite at 0.8, 8.1 and 14.9 GPa. All major peaks can be assigned to qandilite or Ne (pressure medium; denoted by the *asterisks*)

Table 1 Unit-cell parameters of qandilite at high pressure (room *T*)

P (GPa)	*a* (Å)	*V* (Å^3)
0.0001	8.446(2)[b]	602.58(49)
0.4(1)[a]	8.441(2)	601.50(42)
0.8(1)	8.436(2)	600.33(35)
1.5(1)	8.426(2)	598.13(40)
2.2(1)	8.414(2)	595.72(33)
3.1(1)	8.401(2)	592.94(33)
4.1(1)	8.389(2)	590.39(39)
5.0(1)	8.375(2)	587.36(37)
6.1(1)	8.358(2)	583.79(40)
7.1(1)	8.343(2)	580.75(34)
8.1(1)	8.325(2)	576.97(34)
9.3(1)	8.310(2)	573.90(34)
10.4(1)	8.300(2)	571.72(35)
11.3(1)	8.284(2)	568.51(42)
11.7(1)	8.282(2)	568.00(35)
12.9(1)	8.266(2)	564.76(31)
13.8(1)	8.256(2)	562.77(33)
14.9(1)	8.242(2)	559.91(34)

[a] Pressure determined by averaging the values measured before and after collection of synchrotron data; uncertainty of the *P* measurement in the high-*P* experiments assumed as 0.1 GPa

[b] Numbers in parentheses representing one standard deviation

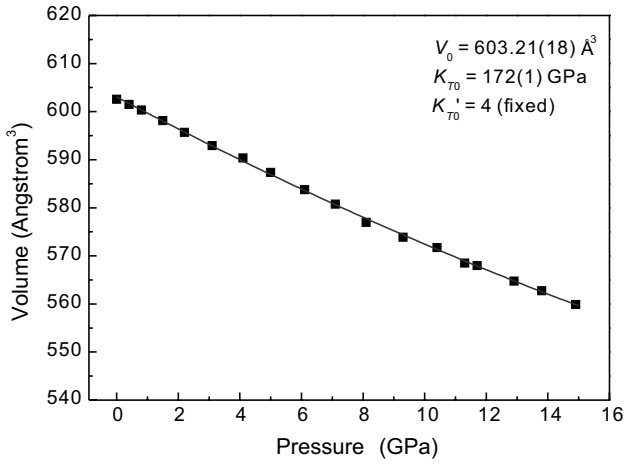

Fig. 3 Effect of pressure on the volume of qandilite at 300 K. *Solid curve* represents the second-order Birch–Murnaghan equation of state, as established in this study. Note that for most data points their *error bars* are approximate to or smaller than the symbols

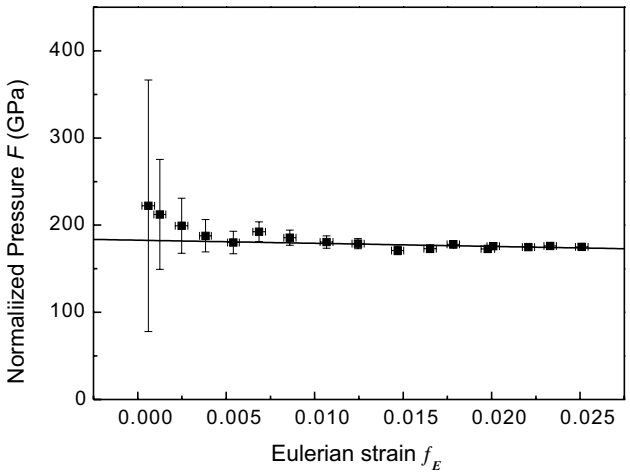

Fig. 4 Eulerian strain-normalized pressure (f_E–F) plot for qandilite. Estimated standard deviations have been calculated following the method in Heinz and Jeanloz (1984). The *solid line* represents a weighted linear fit through the data

of the normalized pressure (F) as a function of Eulerian strain (f_E), i.e., the f_E–F plot (Fig. 4) (Birch 1978). The two variables, F and f_E, are defined as:

$$F = \frac{P}{3f_E(1+2f_E)^{\frac{5}{2}}},$$

and

$$f_E = \frac{1}{2}\left[\left(\frac{V_0}{V}\right)^{\frac{2}{3}} - 1\right].$$

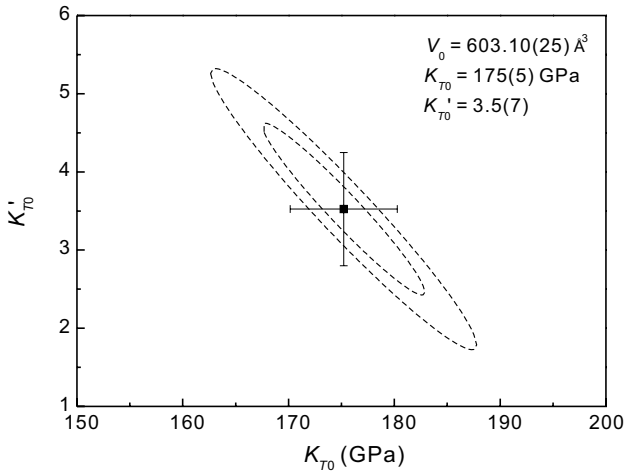

Fig. 5 Confidence ellipse in K_{T0} and K'_{T0} verifies our P–V data fit for qandilite. The inner ellipse is for a 68.3 % confidence level (Chi-square distribution with 2° of freedom $\Delta = 2.30$; see Angel (2000) for details), and the outer one is for a 90 % confidence level ($\Delta = 4.61$). The values of K_{T0} and K'_{T0} determined by the least-squares refinement using the software EoS fit 5.2 (Angel 2000) are also shown. *Error bars* correspond to $\pm 1\sigma$

The third-order Birch–Murnaghan equation of state can then be rewritten as:

$$F = \frac{3}{2}K_{T0}\left(K'_{T0} - 4\right)f_E + K_{T0},$$

so that the slope of the line defined by the experimental data should be equal to $3/2K_{T0}$ $(K'_{T0} - 4)$, and the intercept value is the isothermal bulk modulus. Accordingly, a slope of zero means $K'_{T0} = 4$, a negative slope $K'_{T0} < 4$, and a positive slope $K'_{T0} > 4$. Figure 4 clearly suggests that the K'_{T0} of the qandilite is close to 4, justifying our EoS fit.

The values of the two refined variables K_{T0} and K'_{T0} are strongly correlated (Angel 2000), and this correlation must be evaluated when comparing a set of parameters of the equation of state determined by a least-squares refinement. To visualize the correlation between these parameters, it is usual to make use of a series of confidence ellipses in the parameter space, in which the axes x and y represent the values of K_{T0} and K'_{T0}, respectively (Bass et al. 1981). This approach has been followed in our study. Figure 5 displays the confidence ellipses for the qandilite corresponding to the 68.3 and 90 % confidence levels (see Angel (2000) for details). The ellipses for the qandilite strongly elongate with negative slopes, reflecting the negative correlation between the K_{T0} and K'_{T0} parameters (Fig. 5). The inner ellipse represents an area in which the K_{T0} and K'_{T0} parameters locate to the 68.3 % confidence level (e.g., the probability of the true values of K_{T0} and K'_{T0} to lie in that

Table 2 Isothermal bulk modulus of ulvöspinel and qandilite at ambient P and T

Sample	K_{T0} (GPa)	K'_{T0}	References
Fe_2TiO_4	251(3)[a]	4[b]	Yamanaka et al. (2009, 2013)
Fe_2TiO_4	121(2)[c]	–	Syono et al. (1971)
Fe_2TiO_4	148(4)	4[b]	Xiong et al. (2015)
Mg_2TiO_4	152(7)[c]	–	Liebermann et al. (1977)
Mg_2TiO_4	169[d]	–	Hazen and Yang (1999)
Mg_2TiO_4	172(1)	4[b]	This study
Mg_2TiO_4	175(5)	3.5(7)	This study

[a] Numbers in parentheses representing one standard deviation

[b] Fixed value

[c] Adiabatic bulk modulus, expected to be slightly larger than the corresponding K_{T0}

[d] Empirical estimate

area), and the outer one is for the confidence level of 90 %. Considering the 90 % confidence ellipse, the K_{T0} value of the qandilite can vary in the range 163–188 GPa with the K'_{T0} value spanning 1.7–5.3, which thus verifies our data fitting process.

The K_{S0} of the qandilite was once determined as 152(7) GPa by using an ultrasonic pulse echo method (Liebermann et al. 1977), about 12 % smaller than our K_{T0} value if we ignore the small difference between the K_{S0} and K_{T0}. The primary reason for the relatively small K_{S0} is that the velocity data were taken at pressures up to 0.75 GPa only. As illustrated by Rigden et al. (1988) and Rigden and Jackson (1991), this magnitude of experimental pressure may have led to underestimate of the porosity of the polycrystalline specimen, then underestimate of the velocities, and eventually underestimate of the K_{S0}. On the other hand, our experimentally obtained K_{T0} value is in excellent agreement with the empirical estimate of Hazen and Yang (1999; 169 GPa), which was based on consideration of crystal chemical systematics of the spinels.

Similar to the qandilite, the ulvöspinel is also an inverse 4–2 spinel, with the structural formula of $^{T}(Fe^{2+})^{M}(Fe^{2+}Ti^{4+})O_4$. In spite of a sharp contrast in the values of the bulk modulus among the early experimental determinations (Syono et al. 1971; Yamanaka et al. 2009, 2013; Table 2), the most recent high-P compression experiments accurately constrained its isothermal bulk modulus as ~148(4) GPa (K'_{T0} fixed as 4; Xiong et al. 2015). Therefore, the isothermal bulk modulus of the qandilite is ~16 % larger than that of the ulvöspinel. The exact variation pattern of the isothermal bulk modulus of the spinel solid solutions along the Mg_2TiO_4–Fe_2TiO_4 join is presently unclear though.

The very different isothermal bulk moduli between the qandilite and ulvöspinel are mostly caused by the Mg–Fe substitution on the T sites of the 4–2 spinels. As outlined by their structural formulas, the Mg–Fe substitution occurs on both the T sites and the M sites. Since the variation rates with the change of pressure of the Mg^{2+}–O and Fe^{2+}–O bond lengths on the M sites of the spinels are essentially identical, 47 × 10^{-4} Å/GPa (Hazen and Yang 1999), the effect of the Mg–Fe substitution on the M sites of the spinels on the bulk modulus should be much negligible. As an example, the ringwoodite solid solutions along the Mg_2SiO_4–Fe_2SiO_4 join, normal 4–2 spinels with the Mg–Fe substitution occurring on the M sites only, show little variation in their bulk moduli ($K_{S0} = 185.0(1) + 7.0(1) \times X_{Fe}$, where X_{Fe} is the atomic ratio Fe/(Fe + Mg) of the ringwoodites; Liu et al. 2015). In contrast, the variation rates with the change of pressure of the Mg^{2+}–O and Fe^{2+}–O bond lengths on the T sites are 46 × 10^{-4} Å/GPa and 49 × 10^{-4} Å/GPa, respectively (Hazen and Yang 1999). That is to say, the MgO_4 tetrahedra are relatively harder to compress than the FeO_4 tetrahedra, resulting in a larger isothermal bulk modulus for the qandilite.

Acknowledgments We thank Dr R. J. Angel for the discussions about the EoS fitting procedures, Dr F. Nestola and one anonymous reviewer for their constructive comments on our manuscript, and Dr T. Tsuchiya for processing our paper. The high-P work was performed at GeoSoilEnviroCARS (Sector 13), Advanced Photon Source (APS), Argonne National Laboratory. GeoSoilEnviroCARS is supported by the National Science Foundation-Earth Sciences (EAR-1128799) and Department of Energy-GeoSciences (DE-FG02-94ER14466). Use of the COMPRES-GSECARS gas loading system was supported by COMPRES under NSF Cooperative Agreement EAR 11-57758 and by GSECARS through NSF Grant EAR-1128799 and DOE Grant DE-FG02-94ER14466. This research used resources of the Advanced Photon Source, a U.S. Department of Energy (DOE) Office of Science User Facility operated for the DOE Office of Science by Argonne National Laboratory under Contract No. DE-AC02-06CH11357. This work is financially supported by the Natural Science Foundation of China (Grant Nos. 41440015 and 41273072).

References

Akimoto S, Syono Y (1967) High-pressure decomposition for some titanate spinels. J Chem Phys 47:1813–1817

Al-Hermezi HM (1985) Qandilite, a new spinel end-member, Mg_2TiO_4, from the Qala-Dizeh region, NE Iraq. Miner Mag 49:739–744

Angel RJ (2000) Equation of state. In: Hazen RM, Downs RT (eds) High-temperature and high-pressure crystal chemistry. Reviews in Mineralogy and Geochemistry, vol 41. Mineralogical Society of America, Chantilly, pp 35–60

Bass JD, Liebermann RC, Weidner DJ, Finch SJ (1981) Elastic properties from acoustic and volume compression experiments. Phys Earth Planet Inter 25:140–158

Birch F (1947) Finite elastic strain of cubic crystals. Phys Rev 71:809–924

Birch F (1978) Finite strain isotherm and velocities for single-crystal and polycrystalline NaCl at high-pressures and 300 K. J Geophys Res 83:1257–1268

Bosi F, Hålenius U, Skogby H (2014) Crystal chemistry of the ulvöspinel-qandilite series. Am Miner 99:847–851

Chang L, Chen Z, Liu X, Wang H (2013) Expansivity and compressibility of wadeite-type $K_2Si_4O_9$ determined by in situ high T/P experiments, and their implication. Phys Chem Miner 40:29–40

Ferry JM (1996) Three novel isograds in metamorphosed siliceous dolomites from the Ballachulish aureole, Scotland. Am Miner 81:485–494

Fleet ME, Liu X, Shieh SR (2010) Structural change in lead fluorapatite at high pressure. Phys Chem Miner 37:1–9

Gittins J, Fawcett JJ, Rucklidge JC, Brooks CK (1982) An occurrence of the spinel end-member Mg_2TiO_4 and related spinel solid solutions. Miner Mag 45:135–137

Harrison RJ, Palin EJ, Perks N (2013) A computational model of cation ordering in the magnesioferrite–qandilite ($MgFe_2O_4$–Mg_2TiO_4) solid solution and its potential application to titanomagnetite (Fe_3O_4–Fe_2TiO_4). Am Miner 98:698–708

Hazen RM, Yang H (1999) Effects of cation substitution and order-disorder on *PVT*-equations of state of cubic spinels. Am Miner 84:1956–1960

Heinz DL, Jeanloz R (1984) The equation of state of the gold calibration standard. J Appl Phys 55:885–893

Holland TJB, Redfern SAT (1997) Unit cell refinement from powder diffraction data; the use of regression diagnostics. Miner Mag 61:65–77

Hu X, Liu X, He Q, Wang H, Qin S, Ren L, Wu C, Chang L (2011) Thermal expansion of andalusite and sillimanite at ambient pressure: a powder X-ray diffraction study up to 1000 °C. Miner Mag 75:363–374

Klotz S, Chervin JC, Munsch P, Le Marchand G (2009) Hydrostatic limits of 11 pressure transmitting media. J Phys D Appl Phys 42:075413

Liebermann RC, Jackson I, Ringwood AE (1977) Elasticity and phase equilibria of spinel disproportionation reactions. Geophys J Int 50:553–586

Liu X, Shieh SR, Fleet ME, Zhang L (2009) Compressibility of a natural kyanite to 17.5 GPa. Prog Nat Sci 19:1281–1286

Liu X, Shieh SR, Fleet ME, Zhang L, He Q (2011) Equation of state of carbonated hydroxylapatite at ambient temperature up to 10 GPa: significance of carbonate. Am Miner 96:74–80

Liu X, Xiong Z, Chang L, He Q, Wang F, Shieh SR, Wu C, Li B, Zhang L (2015) Anhydrous ringwoodites in the mantle transition zone: their bulk modulus, solid solution behavior, compositional variation, and sound velocity feature. Solid Earth Sci. doi:10.1016/j.sesci.2015.09.001

Mao HK, Bell PM, Shaner JW, Steinberg DJ (1978) Specific volume measurements of Cu, Mo, Pt, and Au and calibration of ruby R1 fluorescence pressure gauge for 0.006 to 1 Mbar. J Appl Phys 49:3276–3283

Millard RL, Peterson RC, Hunter BK (1995) Study of the cubic to tetragonal transition in Mg_2TiO_4 and Zn_2TiO_4 spinels by ^{17}O MAS NMR and Rietveld refinement of X-ray diffraction data. Am Miner 80:885–896

O'Neill HStC, Scott DR (2005) The free energy of formation of Mg_2TiO_4 (synthetic qandilite), an inverse spinel with configurational entropy. Eur J Miner 17:315–323

O'Neill HStC, Redfern SA, Kesson S, Short S (2003) An in situ neutron diffraction study of cation disordering in synthetic qandilite Mg_2TiO_4 at high temperatures. Am Miner 88:860–865

Oktyabrsky RA, Shcheka SA, Lennikov M, Afanasyeva TB (1992) The first occurrence of qandilite in Russia. Miner Mag 56:385–389

Palin EJ, Walker AM, Harrison RJ (2008) A computational study of order–disorder phenomena in Mg_2TiO_4 spinel (qandilite). Am Miner 93:1363–1372

Pascal ML, Fonteilles M, Boudouma O, Principe C (2011) Qandilite from vesuvius skarn ejecta: conditions of formation and miscibility gap in the ternary spinel-qandilite–magnesioferrite. Can Miner 49:459–485

Prescher C, Prakapenka VB (2015) DIOPTAS: a program for reduction of two-dimensional X-ray diffraction data and data exploration. High Press Res 35:223–230

Rigden SM, Jackson I (1991) Elasticity of germanate and silicate spinels at high pressure. J Geophys Res 96:9999–10006

Rigden SM, Jackson I, Niesler H, Ringwood AE, Liebermann RC (1988) Pressure dependence of the elastic wave velocities from Mg_2GeO_4 spinel to 3 GPa. Geophys Res Lett 15:605–608

Sawada H (1996) Electron density study of spinels: magnesium titanium oxide (Mg_2TiO_4). Mater Res Bull 31:355–360

Syono Y, Fukai Y, Ishikawa Y (1971) Anomalous elastic properties of Fe_2TiO_4. J Phys Soc Jpn 31:471–476

Wechsler BA, Navrotsky A (1984) Thermodynamics and structural chemistry of compounds in the system MgO–TiO_2. J Solid State Chem 55:165–180

Wechsler BA, Von Dreele RB (1989) Structure refinements of Mg_2TiO_4, $MgTiO_3$ and $MgTi_2O_5$ by time-of-flight neutron powder diffraction. Acta Crystallogr B 45:542–549

Xiong Z, Liu X, Shieh SR, Wang F, Wu X, Hong X, Shi Y (2015) Equation of state of a synthetic ulvöspinel, $(Fe_{1.94}Ti_{0.03})Ti_{1.00}O_{4.00}$, at ambient temperature. Phys Chem Miner 42:171–177

Yamanaka T, Mine T, Asogawa S, Nakamoto Y (2009) Jahn-Teller transition of Fe_2TiO_4 observed by maximum entropy method at high pressure and low temperature. Phys Rev B 80:134120

Yamanaka T, Kyono A, Nakamoto Y, Meng Y, Kharlamova S, Struzhkin VV, Mao HK (2013) High-pressure phase transitions of $Fe_{3-x}Ti_xO_4$ solid solution up to 60 GPa correlated with electronic spin transition. Am Miner 98:736–744